Model for the boring of ultraintense lasers into overdense plasmas

Wei Yu,[1,2] M. Y. Yu,[1] J. Zhang,[3] and Z. Xu[2]
[1]*Institut für Theoretische Physik I, Ruhr-Universität Bochum, D-44780 Bochum, Germany*
[2]*Shanghai Institute of Optics and Fine Mechanics, Shanghai 201800, China*
[3]*Department of Physics, University of Oxford, Oxford OX1 3PU, United Kingdom*
(Received 28 April 1998)

A simple piston model for the boring of ultraintense lasers into overdense plasmas is proposed. The hydrodynamic behavior of the laser-irradiated plasma is then determined in a self-consistent manner. Scaling laws for the parameters characterizing the laser penetration, shock propagation, and shock-compressed plasma are presented. [S1063-651X(98)13511-0]

PACS number(s): 52.40.Nk, 52.35.Mw, 52.60.+h, 52.35.Tc

I. INTRODUCTION

In the initial stage of laser interaction with solid targets, a supersonic thermal wave propagates inward with ever decreasing speed. When the thermal wave slows to the order of the ion sound speed, hydrodynamic motion develops and a quasistationary state is rapidly reached [1,2]. The hydrodynamic behavior of a laser-irradiated plasma depends on the ponderomotive and thermal pressures. For lasers of intermediate intensity, the thermal pressure is dominant, the heated plasma ablates backwards into the vacuum along the thermal pressure gradient, while the reacting momentum pushes the plasma inwards and gives rise to a shock [3,4]. Such a picture seems to be consistent with the results [see, for example, Wilks [5], Fig. 4(b), Denavit [6], Fig. 3, and Pukhov and Meyer-ter-Vehn [15], Fig. 1(a)] of numerical simulations where shock and compression regions are seen. Shock generation by plasma ablation has been studied using the rocket model [1,7–10]. With ultraintense lasers, it is possible for the ponderomotive pressure to dominate over the thermal pressure. Instead of flowing outward, the plasma is pushed inward by the light pressure directly. This process, referred to as plasma boring, was first demonstrated in numerical simulations [5,11]. It has attracted much attention [6,12–18] because of its possible application for fast ignition in laser fusion. In the experiments, the propagation speed and direction of the vacuum-plasma interface can easily be measured from the Doppler shift in the spectrum of the reflected light: blueshift for an expanding plasma and redshift for plasma boring [5,14,16,17].

The penetration of laser light into overdense plasmas is confined to a very thin layer of the order of the skin depth. For ultraintense lasers, the light pressure dominates over the thermal pressure, the penetration layer recedes into the target against the light pressure gradient. The recession speed g can be estimated [5,11,14] by balancing the light pressure with the momentum flux of the inward-streaming plasma. One obtains $K \equiv g/c = q\sqrt{(Zm/m_i)(n_c/n)} = 0.012q\sqrt{n_c/n}$, where m and m_i are the electron and ion masses, Z is the ion charge number, n_c and n are the critical and electron densities, $q = e|E_L|/m\omega c = 0.85\times 10^{-9}\lambda\sqrt{I}$ is the laser strength parameter, $I = (c/8\pi)|E_L|^2$ is the laser intensity in units of W/cm^2, and λ is the laser wavelength in μm. However, this estimate yields no information on the inward-streaming plasma flow, which determines [3,4] the properties of the shock. Nevertheless, using available measured parameter values, useful information about the shock can be obtained. Accordingly, Denavit [6] associated the shock and soliton structures observed in the simulations with the well-known electrostatic ion acoustic solitons and ''collisionless'' Sagdeev shocks [4]. The measured soliton and shock speed ranges for these structures seem to agree with that from theory [4,6]. On the other hand, a self-consistent theory including the relation between the laser-plasma interaction parameters and the upstream flow speed would be of practical interest.

Physically, one may imagine that the ultraintense laser pushes into the plasma like a piston [12,13,18]. The plasma in the penetration layer is then set into motion, its momentum passes inward and gives rise to a shock when the flow becomes locally supersonic. Here we propose a modified piston model to describe the interaction region. The model consists of an undisturbed plasma in front of the shock and a shock-compressed platform of uniform density and temperature behind it. The penetration layer is attached to the outer edge of the platform. With this model, the behavior of the plasma and the laser can be determined self-consistently. The results for the parameters characterizing the laser penetration, the shock propagation, and the shock-compressed plasma can be useful in the design and diagnostics of experiments involving ultraintense laser interaction with overdense plasmas.

II. FORMULATION

For simplicity, we shall assume that the dimension of laser focus spot is larger than that of the compressed plasma, so that the plasma motion can be taken as one dimensional. In a frame moving with the penetration layer, the conservation equations can be written in normalized units as

$$d_\xi(NV') = 0, \tag{1}$$

$$Nd_\xi\gamma_0 = T(V'^2 - 1)d_\xi N, \tag{2}$$

$$d_\xi^2 a + (1 - N/\gamma_0)a = 0, \tag{3}$$

where $\xi = \omega z/c$, $N = n/n_c$, $V' = v'/s$, $\gamma_0 = (1 + a^2/2)^{1/2}$, $a = e|E|/m\omega c$, E is the electric field strength, $v' = v - g$ is the

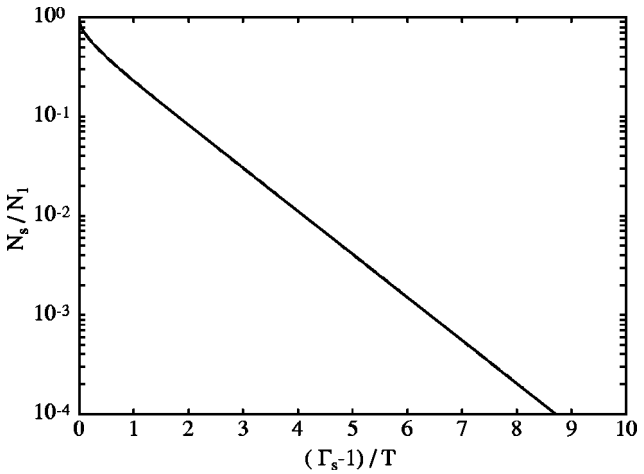

FIG. 1. The density N_s/N_1 at the sonic point as a function of $(\Gamma_s-1)/T$. Here $(\Gamma_s-1)/T$ is the ratio of the electron quiver energy to thermal energy.

plasma flow speed in the moving frame, $s/c=\sqrt{ZTm/m_i}$ is the normalized (by the light speed c) ion sound speed, and T is the plasma temperature normalized by mc^2. For the time scale under consideration, thermal conduction, which is of the order of the electron thermal speed, readily smoothes out any local temperature difference. Thus the plasma behind the shock front can be taken as isothermal. In the nonrelativistic limit, Eqs. (1)–(3) reduce to that for treating plasma ablation [1,7,9,10] associated with less intense lasers.

The density profile in the penetration layer is characterized by a very steep gradient connecting the upper and lower density shelves. We see from Eq. (2) that the laser radiation peaks at the sonic point, where $V'=1$, $N=N_s$, and $\gamma_0=\Gamma_s$.

Equations (1)–(3) can easily be solved to yield

$$V'=N_s/N, \tag{4}$$

$$(\Gamma_s-\gamma_0)/T=(N_s^2/N^2-1)/2-\ln(N_s/N), \tag{5}$$

$$\gamma_0^2(d_\xi\gamma_0)^2=(\gamma_0^2-1)[(\Gamma_s^2-\gamma_0^2)-2NT(N_s/N-1)^2] \tag{6}$$

for the penetration layer. The laser field decays (i.e., a and $d_\xi a$ tend to zero) at the upper density shelf where $N=N_1$ and $V'=V_1'$. From Eqs. (4)–(6) one obtains

$$(\Gamma_s-1)/T=(N_s^2/N_1^2-1)/2-\ln(N_s/N_1), \tag{7}$$

$$(\Gamma_s^2-1)/T=2N_1(N_s/N_1-1)^2 \tag{8}$$

for the upper density shelf.

In Fig. 1, N_s/N_1 is plotted as a function of the ratio $(\Gamma_s-1)/T$ of electron quiver energy to the thermal energy. For ultraintense lasers the quiver energy is much higher than the thermal energy, and that makes N_s/N_1 very close to zero. As a result, the density jump can be treated as a vacuum-plasma interface and in this approximation the sonic point is actually located on the vacuum side. From the boundary condition we then have $\Gamma_s^2-1=2q^2$, and Eqs. (8) becomes

$$N_1T=q^2=2I/n_cmc^3, \tag{9}$$

which simply says that in the moving frame the light and thermal pressures are in balance.

III. RESULTS

We now evaluate the parameters of interest. The parameters in the upper shelf of the density jump are related to those of the shock-compressed platform. To study the shock front, we stay in the frame moving with the penetration layer and express the Hugoniot relations [1,3] as

$$\eta(V_1'-F')=(V_0'-F'), \tag{10}$$

$$\eta[1+(V_1'-F')^2]=T_0/T+(V_0'-F')^2, \tag{11}$$

$$5+(V_1'-F')^2=5(T_0/T)+(V_0'-F')^2, \tag{12}$$

where $\eta=N_1/N_0$ is the compression ratio, $N_0=n_0/n_c$, $V_0'=v_0'/s$, $F'=f'/s$, n_0 is the electron density in the undisturbed plasma, and f' and v_0' are the speeds (in the moving frame) of the shock and the undisturbed plasma, respectively. From Eqs. (10)–(12) we obtain

$$F'=V_1'+\sqrt{5/(4\eta-1)}, \tag{13}$$

$$V_0'=V_1'-(\eta-1)\sqrt{5/(4\eta-1)}, \tag{14}$$

$$T_0/T=\eta(4-\eta)/(4\eta-1) \tag{15}$$

for the normalized shock speed, the flow speed, and the temperature.

From Eqs. (13)–(15) the well-known relation $1\leqslant\eta<4$ for planar shocks can be recovered. The speeds can be transformed to the laboratory frame through the relations $V=V'+G$ and $F=F'+G$. In the laboratory frame where the undisturbed plasma is at rest the recession speed is $G=g/s=-V_0'$.

Equation (9) gives $T=q^2/N_0\eta$ and $s/c=K/\sqrt{\eta}$ for the temperature of the shock-compressed plasma and the corresponding ion sound speed, and $K=0.012q/\sqrt{N_0}$. Equations (13) and (14) yield

$$g/c=(\eta-1)\sqrt{5/\eta(4\eta-1)}K, \tag{16}$$

$$f/c=\sqrt{5\eta/(4\eta-1)}K \tag{17}$$

for the recession and shock speeds.

Since the compression ratio η is confined to a limited range, the above equations yield rather good scalings even when the exact value of the compression ratio is unknown. In Fig. 2 the temperature (in units of keV) of the compressed plasma is plotted as a function of q^2/N_0. The solid and dashed curves correspond to $\eta=1$ and 4, respectively. In general, all speeds involved in the hydrodynamic process are of the order of the ion sound speed [3]. In fact, both the shock speed and the ion sound speed scale with K. Furthermore, the shock Mach number $M_s=f/s=\eta\sqrt{5/(4\eta-1)}$ depends only on η and has the range 1.29–2.31, which is consistent with that from the simulations [6] for low-Z ions. This range is relevant to the ''collisionless'' Sagdeev [4,6] and envelope [7] shocks.

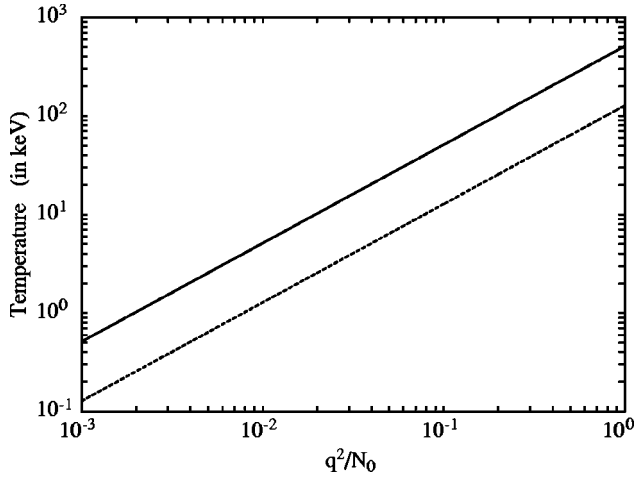

FIG. 2. The temperature (in keV) of the shock-compressed plasma as a function of q^2/N_0. The two curves correspond to $\eta=1$ (solid) and 4 (dotted), respectively.

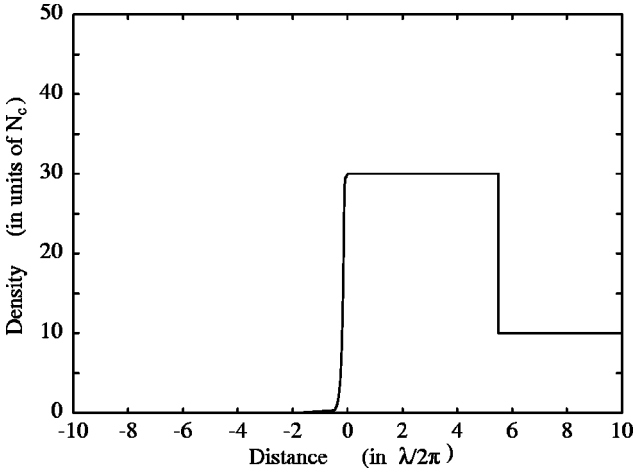

FIG. 3. The profile of the laser-irradiated plasma for $I\lambda^2=10^{19}$ W μm^2 cm^{-2}, $\tau=1$ psec, $N_0=n_0/n_c=10$, and $\eta=3$. Here, $k=2\pi/\lambda$, where λ is the laser wavelength.

The depth of the penetration layer can be represented by the scale length at the critical density where $N=1$, $V'=N_s$, and $\gamma_0=\Gamma_c$. From Eq. (2) we have $kL_c=|N/d_\xi N|_{\xi_c}$, or

$$kL_c=(q^2\Gamma_c/N_1)\sqrt{(\Gamma_c^2-1)(\Gamma_s^2-\Gamma_c^2)}, \tag{18}$$

where $\Gamma_c=1+(q^2/N_1)\ln N_1$ and $k=\omega/c$. The depth of the plasma platform is approximately

$$d=(f-g)\tau=c\tau\sqrt{5/\eta(4\eta-1)}K, \tag{19}$$

where τ is the pulse duration.

In the earlier studies [8] on shock generation by plasma ablation, the temperature ahead of the shock is assumed to be known (usually a sufficiently low temperature) and then the compression ratio is determined. This approach is clearly not suitable for the present problem. For normal incidence of a linearly polarized laser, the $\mathbf{J}\times\mathbf{B}$ heating is the main mechanism of laser absorption, which produces energetic electrons directed into the target [11]. With ranges much larger than the depth of the shock-compressed plasma, these electrons travel ahead of the shock and deposit most of their energy by preheating the initially cold material [8,11]. The preheating involves a variety of physical processes, and it is thus difficult to estimate the plasma state ahead of the shock. On the other hand, the compression ratio η can be determined by measuring the recession velocity or the surface temperature. Equation (14) then gives

$$T_0=q^2(4-\eta)/N_0(4\eta-1) \tag{20}$$

for the temperature ahead of the shock.

IV. DISCUSSION

The boring of an ultraintense laser into a plasma is associated with a new mechanism of laser absorption [18]. Here the radiation reflected from the receding plasma interface is Doppler redshifted by $\delta\omega/\omega=2g/c$. Thus, even if all the incident photons are reflected, a finite amount of laser energy, $I_{\rm abs}=(I/\hbar\omega)\hbar\,\delta\omega=2(g/c)I$, where $I/\hbar\omega$ is the flux photon number, is absorbed by the plasma. In terms of the piston model, noting that the work done by the light pressure is $2I/c$ per unit time, one also obtains $I_{\rm abs}=2(g/c)I$ for the absorption. Although the absorption rate is not large, the absorbed energy is more than sufficient to account for the heating of the compressed plasma.

Plasma boring can occur in the interaction of an intense laser pulse with preplasmas as well as solid targets. In the experiments, preplasmas can be produced by a separate laser pulse, a prepulse ahead of the main peak, or the rise front of a not-so-clean laser pulse. Typically, the size of a preplasma is a few laser wavelengths or more. In this case N_0 is the average preplasma density, which is well below the solid-target density but still overcritical. The laser can easily push into the preplasma and results in a larger redshift in the reflected light than that for a clean pulse-solid target interaction. For $I\lambda^2=10^{19}$ W μm^2 cm^{-2}, $\tau=1$ psec, $N_0=10$, and $\eta=3$, the plasma density profile is shown in Fig. 3. The temperatures behind and ahead the shock are 120 keV and 33 keV, respectively. The recession and shock speeds are $0.008c$ and $0.012c$ (corresponding to $M_s=2.02$), respectively. The depth of laser penetration is $L_c=0.37\lambda$, and depth of the compressed plasma is $d=1.2$ μm.

One can also apply the present model to the boring of solid targets by a ''clean'' laser pulse, i.e., a pulse with a very sharp rising front. Such a pulse can push into the solid-density plasma directly if its intensity is sufficiently high. In this case N_0 is the normalized electron density of the target. The spatial structure is similar to that of Fig. 3 for interaction with a preformed plasma discussed above, but the scales for both the temperature and distance are much reduced here. For $I\lambda^2=10^{19}$ W μm^2 cm^{-2}, $\tau=1$ psec, $N_0=300$ (or mass density $\rho\approx 1$ g cm^{-3}), and $\eta=3$, the temperature of the compressed plasma is merely 4 keV. With $K=0.0019$, the recession and shock speeds are of the order $10^{-3}c$. The depth L_c of laser penetration is 0.01λ, and the depth d of the compressed plasma is 0.22 μm.

To summarize, we have presented in this paper a simple one dimensional model for the boring into overdense plasmas by ultraintense lasers. The model is based on the observation that the plasma in the laser penetration layer is pushed

inward by the light pressure [5,6]. A shock is then formed when the flow becomes sufficiently high locally. The present situation differs from that [1,7–10] for weaker lasers in that here the light pressure greatly dominates over the thermal pressure. Parameters of physical interest are then obtained self-consistently. The results may be useful in predicting the penetration depth, the shock Mach number, the temperature and size of the compressed plasma, etc. The model, which is based on quasi-stationary hydrodynamic conservation laws, does not describe the details of the process. In particular, it does not account for the ultrafast electrons observed in the simulations and experiments [5,12,19]. These electrons are, however, few in number and have very long stopping distances, and are therefore not expected to directly affect the region of interest. On the other hand, the model is one dimensional, so that several related important phenomena [14–18,20,21], such as self-focusing of the laser light, channel formation in the plasma, and magnetic field generation, are precluded.

ACKNOWLEDGMENTS

This work was partially supported by the Sonderforschungsbereich 191 Niedertemperatur Plasmen. One of the authors (W.Y.) thanks the K. C. Wong Education Foundation (Hong Kong), the Deutscher Akademischer Austauschdienst, and the National High-Technology Program of China (Contract No. 863-416-3-1-4) for financial support.

[1] C. E. Max, Lawrence Livermore National Laboratory Report UCRL-53107, 1981, and the references therein.
[2] R. Pakula and R. Sigel, Phys. Fluids **28**, 232 (1985).
[3] Ya. B. Zel'dovich and Yu. P. Raiser, *Physics of Shock Waves and High Temperature Hydrodynamic Phenomena* (Academic, New York, 1966).
[4] D. A. Tidman and N. A. Krall, *Shock Waves in Collisionless Plasmas* (Wiley-Interscience, New York, 1971).
[5] S. C. Wilks, Phys. Fluids B **5**, 2603 (1993).
[6] J. Denavit, Phys. Rev. Lett. **69**, 3052 (1992).
[7] K. Lee *et al.*, Phys. Fluids **20**, 51 (1977).
[8] R. J. Trainor and Y. T. Lee, Phys. Fluids **25**, 1898 (1982).
[9] R. Fabbro *et al.*, Phys. Fluids **28**, 1463 (1985).
[10] W. Yu *et al.*, J. Phys. D **29**, 1515 (1996).
[11] S. C. Wilks, W. L. Kruer, M. Tabak, and A. B. Langdon, Phys. Rev. Lett. **69**, 1383 (1992).
[12] R. N. Sudan, Phys. Rev. Lett. **70**, 3075 (1993).
[13] E. G. Gamaly, Laser Part. Beams **12**, 185 (1994).
[14] M. Zepf *et al.*, Phys. Plasmas **3**, 3242 (1996).
[15] A. Pukhov and J. Meyer-ter-Vehn, Phys. Rev. Lett. **79**, 2686 (1997).
[16] J. Fuchs *et al.*, Phys. Rev. Lett. **80**, 2326 (1998).
[17] S. Y. Chen, G. S. Sarkisov, A. Maksimchuk, R. Wagner, and D. Umstadter, Phys. Rev. Lett. **80**, 2610 (1998).
[18] S. C. Wilks, W. L. Kruer, and W. B. Mori, IEEE Trans. Plasma Sci. **21**, 120 (1993).
[19] Wei Yu, M. Y. Yu, Z. M. Sheng, and J. Zhang, Phys. Rev. E **58**, 2456 (1998).
[20] D. Teychenne, A. Giulietti, D. Giulietti, and L. A. Gizzi, Phys. Rev. E **58**, 1245 (1998).
[21] A. R. Bell, J. R. Davies, and S. M. Guerin, Phys. Rev. E **58**, 2471 (1998).